Deep Unfolding RPCA for High-Resolution Flow Estimation

Vassili Pustovalov, Duong-Hung Pham, Denis Kouamé

Deep Unfolding RPCA for High Resolution Flow Estimation

Vassili Pustovalov, Duong Hung Pham, Denis Kouame
Université Paul Sabatier (Toulouse III), IRIT, CNRS UMR 5505, Toulouse, France

***Abstract*—Numerous techniques have been proposed to produce high precision blood flow or contrast-enhanced ultrasound estimates from fast ultrasound sequences. Among them, robust principal component analysis (RPCA)-based methods are known as superior to most state-of-the-art techniques. In particular, these techniques may include a deconvolution step which allows for further improvement of the resolution of the estimated blood flow images. However, they rely on many hyperparameters that have to be manually adjusted to obtain the optimal solution. To overcome this limitation, we propose a new deep unfolding neural network based on the DRPCA iterative algorithm, which enables the reconstruction of high-resolution and high-sensitivity blood flow components. Compared to other state-of-the-art methods, the proposed algorithm showed interesting performances, in terms of PSNR and SSIM on simulation data.**

***Index Terms*—Blind Deconvolution (BD), Blood Flow, Clutter Separation, Robust Principal Component Analysis (RPCA), Power Doppler, High Resolution**

I. Introduction

In ultrafast ultrasound imaging and contrast-enhanced ultrasound imaging, the problem of reconstructing the blood flow and removing clutter signals from the raw data has received great interest from the community. For example, iterative RPCA-based techniques consist in formulating a mathematical model of the data and then finding a solution by optimizing the problem related to this model [10], [13]. This allows the use of regularizations, for example, blood sparsity or tissue low rank, in order to leverage prior knowledge for an efficient blood flow reconstruction. To further improve the reconstruction, a deconvolution step was recently introduced in the RPCA framework [1], [2]. This approach called deconvolved RPCA (DPRCA) involves recovering the tissue reflectivity function from the observed data using a measured or estimated point spread function (PSF).

As mentioned above, all these methods are based on iterative optimization algorithms to find the solution such as the alternating direction method of multipliers (ADMM), Backward-Forward, Douglas-Rachford, iterative shrinkage-thresholding algorithm (ISTA), etc [10] [14] [15]. However, the clinical applicability of these algorithms is limited due to the manual tuning of the hyperparameters and the number of iterations required to achieve the desired result. Alternatively, deep convolutional neural networks (CNNs) have been applied to ultrasound imaging and have shown higher performance than the optimization methods [9]. However, these methods act as block-box engines which limits their interpretability. To deal with all these issues, the unfolding (or unrolling) approaches are increasingly used as they provide a framework for expressing iterative algorithms as neural networks [4] - [8]. More precisely, each iteration step of an iterative algorithm is converted into a single layer of a network, set of which forms a deep CNN. Many unfolding algorithms have been proposed, among which the CORONA algorithm based on an unfolding of the ISTA, enables to efficiently separate the micro-bubbles blood signals from the tissue signals [3].

In this work, we derive the DRPCA algorithm by interpreting the iterations of its ADMM steps as an unfolding CNN that we call as DRPCANet in the sequel. However, unlike CORONA [3], the PSF of the system is explicitly included in the deep unfolding to achieve a high-resolution flow estimation. The remainder of the paper is structured as follows. After having recalled the DRPCA algorithm and its multiple-step ADMM in Section II, we show how to unfold this algorithm to build an unfolded CNN in Section III. Finally, we compare the proposed approach with the CORONA and the iterative DRPCA in Section V.

II. DRPCA algorithm

A. RPCA model

The RPCA problem consists in recovering a low-rank matrix and a sparse matrix from a noisy observation [11]. In our case, we consider that the observation matrix corresponds to the acquired ultrafast ultrasound (US) sequence, which we denote S. The first step consists in rearranging the 3D ultrafast US acquisition into a 2D matrix, called Casorati matrix. This matrix corresponds to a spatio-temporal representation of the acquisition, in which each column is a vectorized frame of the US sequence. Denoting B the sparse matrix, T the low-rank matrix and N the noise matrix associated with the observation, the observation model is:

$$S = B + T + N. \tag{1}$$

In the reconstruction of blood flow problem, it is assumed that the tissue component is motionless. Then, due to space-time invariance, in its Casorati form, all the columns of the tissue matrix are correlated. Therefore, the tissue matrix is assumed to have a low rank and thus corresponds to T. Regarding the blood, since the number of blood vessels is much lower than that of tissues, the blood is assumed to be sparse and as such, corresponds to the B matrix. Thus, the

This work was partly funded by France Life Imaging (FLI) (grant ANR-11-INBS-0006).

solutions to the RPCA problem correspond to the tissue and blood flow matrices [10], [11].

B. A new algorithm for the DRPCA model

To improve the resolution of the reconstructed blood flow, we incorporated a convolution in the RPCA model [1], [2]. More precisely, we considered $B = Hx$ where H denotes the system PSF and x the high-resolution blood flow to be estimated. For computational efficiency, H is assumed to be block circulant with circulant blocks [16].

In [1], [2], we proposed a DRPCA algorithm to recover the deconvolved high-resolution blood flow based on the above model. However, this algorithm requires strong conditions for its convergence. In this paper, we propose a new version of the DRPCA algorithm which enables an easier unfolding later. Before going into the details of this algorithm, we recall the general ADMM framework [14].

Let f and g be convex, closed, and proper functions, ADMM can be used to solve the following minimization problem:

$$\begin{aligned} &\text{minimize} \quad f(\hat{x}) + g(\hat{z}) \\ &\text{subject to} \quad A\hat{x} + B\hat{z} = c. \end{aligned} \tag{2}$$

By minimizing the augmented Lagrangian:

$$\begin{aligned} &L(\hat{x}, \hat{z}, \gamma) = \\ &f(\hat{x}) + g(\hat{z}) + \frac{\rho}{2} \left\| A\hat{x} + B\hat{z} - c + \frac{\gamma}{\rho} \right\|_2^2 + cst\,. \end{aligned} \tag{3}$$

Which general solution is:

$$\hat{x}^{k+1} = \arg\min_{\hat{x}} f(\hat{x}^k) + \frac{\rho}{2} \left\| A\hat{x}^k + B\hat{z}^k - c + \frac{\gamma^k}{\rho} \right\|_2^2, \tag{4}$$

$$\hat{z}^{k+1} = \arg\min_{\hat{z}} g(\hat{z}^k) + \frac{\rho}{2} \left\| A\hat{x}^k + B\hat{z}^k - c + \frac{\gamma^k}{\rho} \right\|_2^2, \tag{5}$$

$$\gamma^{k+1} = \gamma^k + (A\hat{x}^{k+1} + B\hat{z}^{k+1} - c). \tag{6}$$

To separate the high-resolution blood x and the tissue T from S, we use ADMM to solve the following problem:

$$\begin{aligned} [\tilde{x}, \tilde{T}] = \arg\min_{x,T} \frac{1}{2} \left\| S - Hx - y \right\|_F^2 + \lambda \left\| x \right\|_1 + \mu \left\| y \right\|_* \\ \text{such that: } x = Z, y = T, \end{aligned} \tag{7}$$

where Z and y are auxiliary variables. λ, μ are two positive hyperparameters balancing the trade-off between blood sparsity and tissue low rank. $\| \cdot \|_F^2$ is the Frobenius norm, $\| \cdot \|_1$ is the l_1 norm, and $\| \cdot \|_*$ is the nuclear norm. The nuclear norm corresponds to the l_1 norm of the vector of singular values of the considered matrix, thus it favors the appearance of zero singular values in the matrix T, and by extension, it favors a low rank. The l_1 norm favors the sparsity of x.

In order to match (2) with our problem in (7) we define:

$$M_1 = \begin{bmatrix} H & I \end{bmatrix};\ M_2 = \begin{bmatrix} I & 0 \end{bmatrix};\ M_3 = \begin{bmatrix} 0 & I \end{bmatrix};$$

$$\hat{x} = \begin{bmatrix} x \\ y \end{bmatrix};\ \hat{z} = \begin{bmatrix} Z \\ T \end{bmatrix};\ \gamma = \begin{bmatrix} \gamma_1 \\ \gamma_2 \end{bmatrix};$$

Our equality constraint is $\hat{x} - \hat{z} = 0$ and we can choose:

$$f(\hat{x}) = \frac{1}{2} \left\| S - M_1\hat{x} \right\|_F^2,$$

$$g(\hat{z}) = \lambda \left\| M_2\hat{z} \right\|_1 + \mu \left\| M_3\hat{z} \right\|_*.$$

In this way, it is possible to separate the equations (4) to (6) in x and T (or their associated intermediate variables Z and y). And the solution of (7) is obtained by repeating the following iterative step:

$$y^{k+1} = (1+\rho)^{-1}[S - Hx^k + \rho T^k - \gamma_2^k], \tag{8}$$

$$x^{k+1} = (H^T H + \rho I)^{-1}[H^T(S - y^k) + \rho Z^k - \gamma_1^k], \tag{9}$$

$$T^{k+1} = SVT_{\frac{\mu}{\rho}}(y^{k+1} + \gamma_2^k/\rho),$$

$$Z^{k+1} = Soft_{\frac{\lambda}{\rho}}(x^{k+1} + \gamma_1^k/\rho),$$

$$\gamma_1^{k+1} = \gamma_1^k + \rho(y^{k+1} - T^{k+1}),$$

$$\gamma_2^{k+1} = \gamma_2^k + \rho(x^{k+1} - Z^{k+1}),$$

where $Soft_{\frac{\lambda}{\mu}}(x)$ is the soft-thresholding function and SVT is the singular value thresholding function. The variable ρ is a positive penalty parameter that has an influence on the convergence speed, it is set equal to 1 in our case. In the following, we denote by P_1, P_2 and P_3, the three H dependent terms in (8) and (9):

$$P_1 = -H;$$

$$P_2 = (H^T H + \rho I)^{-1};$$

$$P_3 = (H^T H + \rho I)^{-1} H^T;$$

We thus obtained the iterative solution of the new DRPCA algorithm. The variables $\hat{x}$, $\hat{z}$ and γ are initialized as zero. After N iterations, the estimated solution of (7) is $[x^N, T^N]$.

III. Unfolding DRPCA

The iterative solution is unfolded into a multiple-layer neural network where each layer corresponds to an iteration of the DRPCA algorithm. To perform this conversion, we transform the matrix multiplications by P_1, P_2 and P_3 into convolutional layers. Thus, in the unfolded algorithm, we replace P_1, P_2 and P_3 with 2D convolutional kernels. Their weights are learned independently for each layer in a supervised manner. By doing so, the neural network learns to perform the deconvolution of the blood component without the knowledge of the PSF.

In addition, the regularization hyperparameters λ and μ are converted into learnable parameters of the network, they are also learned independently for each layer in a supervised manner. The soft-thresholding and the singular value thresholding operations are performed identically to the iterative DRPCA. The rest of the unfolding is straightforward as only elementary operations remain.

Thereby, we obtain a single layer derived from an iteration of the DRPCA algorithm. The diagram of this layer is given in Fig. 1. The overall neural network, referred to as DRPCANet, is obtained by concatenating several of these layers.

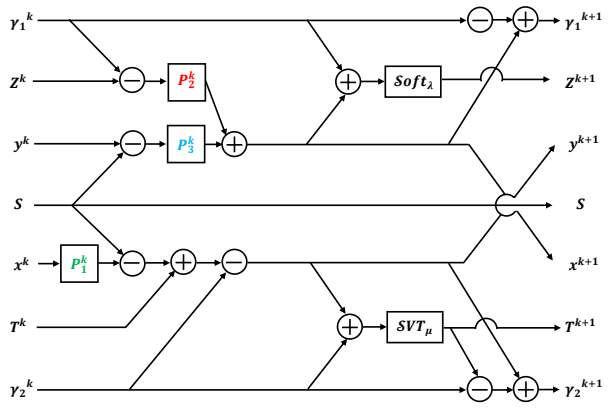

Fig. 1. Single Layer Diagram

DRPCANet was implemented in Python (PyTorch) using its automatic differentiation framework for training. It consists of 20 layers. We trained the network over 400 simulated US sequences (see Section IV), 300 sequences were used for training and 100 for performance assessment. The loss function was a weighted sum of the mean squared errors between the predicted $[x^N, T^N]$ elements and their ground truth. DRPCANet was trained using the Adam optimizer for 100 epochs with a learning rate of 0.01 and a batch size fixed equal to 25. The experiments were performed on a high computation server with 32 GB RAM and 4 GTX-1080-TI GPUs.

During the training, we initialize the sparsity parameter λ as zero and the low-rank parameter μ equal to 5. The actual thresholding values for the soft-thresholding operations is $\sigma(\lambda) = 1/(1 + exp(-\lambda))$ which is the sigmoid of λ. We use the sigmoid function because we observe that it increases stability during training, especially when the hyperparameters are badly initialized.

IV. Simulation Data

In order to make a fair comparison with CORONA [3], we used their code to generate the US image sequences with slight changes to match our model. Compared to the original data, we doubled the tissue amplitude, changed the size of the PSF to be odd, and used only the real part of the data.

We can summarize the data simulation as follows. The ground truth of the blood component is represented by contrast agents (CAs) identified as bubbles. The number of contrast agents, their initial positions and their trajectories are random. The magnitude of the CAs are drawn from a normal distribution. The ground truth of the tissue is created from a mixture of Gaussians. The result is then post-processed and filtered to add a low motion. Finally, the sum of the tissue and CAs is convolved by the PSF and a Gaussian noise is added with a signal-to-noise ratio of 30dB.

We generated a total of 400 image-sequences of size 128×128 pixels and each composed of 50 frames. In Fig. 2 (a) and Fig. 3 (a), we show the raw data. In the next image we show the ground truth of the CAs (Fig. 2 (b) and Fig. 3 (b)). Fig. 2 depicts the Bmode a single frame of the US sequence while Fig. 3 shows the Power Doppler flow.

V. Results

In this section, we provide reconstruction results for DRPCANet trained and tested on the simulated data. Fig. 2 and Fig. 3 present blood flow reconstruction results of the different methods against the ground truth image. Respectively, Fig. 2 (c) and Fig. 3 (c) are the CAs and Power Doppler obtained with the state-of-the-art CORONA neural network, Fig. 2 (d) and Fig. 3 (d) are the CAs and Power Doppler obtained with the iterative DRPCA algorithm, Fig. 2 (e) and Fig. 3 (e) are the CAs and Power Doppler obtained with DRPCANet. The CORONA network performs worse than our algorithms mainly because it does not perform deconvolution. Nevertheless, CORONA manages to separate the CAs from the tissue. As for DRPCA, both the iterative and the unfolded version achieved very clean results.

We compare our approach quantitatively using peak signal-to-noise ratio (PSNR) and multiscale structural similarity (SSIM3) measurements on estimated CAs (Bubbles) in Tab. I. One can see that the unfolded DRPCA network outperforms the other algorithms by a large margin. As our approach differentiates by learning the deconvolution, we also trained CORONA on deconvolved data, but the results obtained were worse than the initial ones.

TABLE I
PSNR and SSIM comparison for the estimations of Fig. 3.

	CORONA [3]	**DRPCA [1]**	**DRPCAnet (Ours)**
PSNR (dB)	24.41	30.32	36.17
SSIM3	0.13	0.71	0.94

VI. Conclusion

Combining a model for the separation problem with a data-driven approach leads to improved separation of blood and tissue signals, together with noise reduction compared to popular optimization approaches. However, unlike CORONA, the PSF of the system is explicitly included in our deep unfolding process making the results more interpretable. Moreover, for DRPCANet, up to twenty layers have proven to be sufficient

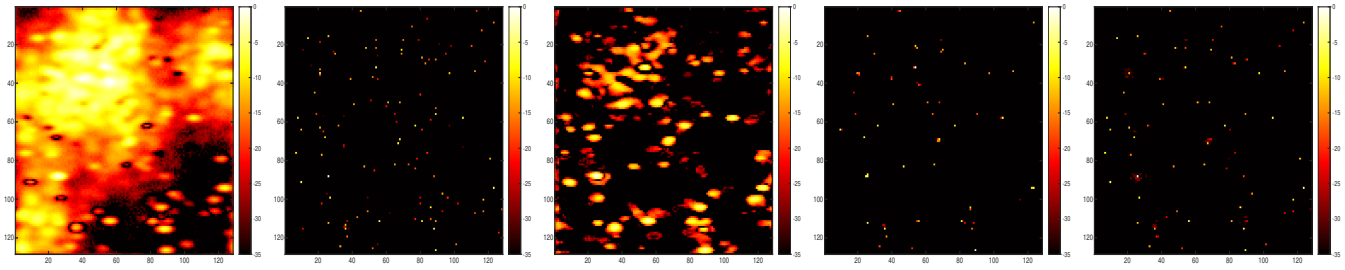

(a) US Data (b) Ground Truth (c) Corona (d) DRPCA ADMM (e) DRPCANet

Fig. 2. Bmodes of a single frame of the estimated sequences of the blood component.

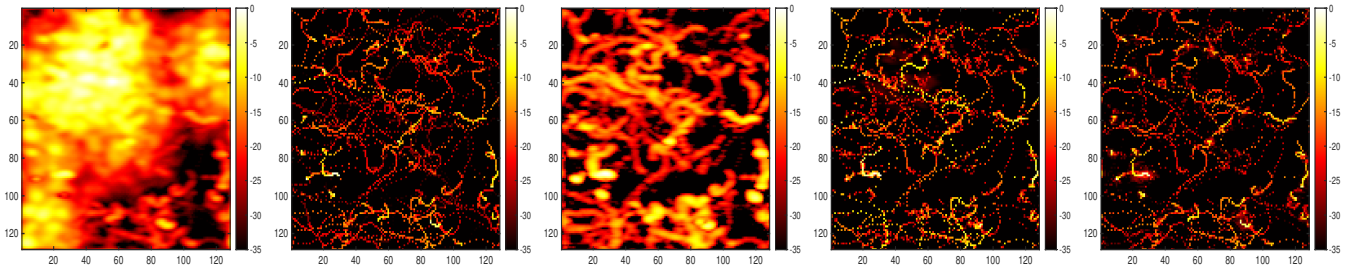

(a) US Data (b) Ground Truth (c) Corona (d) DRPCA ADMM (e) DRPCANet

Fig. 3. Power Doppler images of the estimated blood component from the simulated data.

whereas the iterative DRPCA method requires a hundred iterations to achieve a similar result.

REFERENCES

[1] H. Shen et al., "High-resolution and high-sensitivity blood flow estimation using optimization approaches with application to vascularization imaging," IEEE Int. Ultrason. Symp. (IUS), 2019, pp. 467-470.

[2] D. H. Pham, A. Basarab, I. Zemmoura, J. -P. Remenieras and D. Kouamé, "Joint Blind Deconvolution and Robust Principal Component Analysis for Blood Flow Estimation in Medical Ultrasound Imaging," in IEEE Trans. Ultrason. Ferroelectr. Freq. Control, vol. 68, no. 4, pp. 969-978, April 2021.

[3] O. Solomon et al., "Deep Unfolded Robust PCA With Application to Clutter Suppression in Ultrasound," in IEEE Trans. Med. Imaging, vol. 39, no. 4, pp. 1051-1063, April 2020.

[4] Y. Yang, J. Sun, H. Li and Z. Xu, "ADMM-CSNet: A Deep Learning Approach for Image Compressive Sensing," in IEEE Trans. Pattern Anal. Mach. Intell., vol. 42, no. 3, pp. 521-538, 1 March 2020.

[5] V. Kouni, G. Paraskevopoulos, H. Rauhut and G. C. Alexandropoulos, "ADMM-DAD Net: A Deep Unfolding Network for Analysis Compressed Sensing," IEEE Int. Conf. Acoust. Speech Signal Process. (ICASSP), 2022, pp. 1506-1510.

[6] Y. Li, M. Tofighi, J. Geng, V. Monga and Y. C. Eldar, "Efficient and Interpretable Deep Blind Image Deblurring Via Algorithm Unrolling," in IEEE Trans. Comput. Imaging, vol. 6, pp. 666-681, 2020.

[7] H. Van Luong, B. Joukovsky, Y. C. Eldar and N. Deligiannis, "A Deep-Unfolded Reference-Based RPCA Network For Video Foreground-Background Separation," 2020 28th European Signal Processing Conference (EUSIPCO), 2021, pp. 1432-1436.

[8] Juan Marcos Ramirez, José Ignacio Martínez-Torre, Henry Arguello, "LADMM-Net: An unrolled deep network for spectral image fusion from compressive data ", Signal Processing, Volume 189, 2021, pp. 108-239, ISSN 0165-1684.

[9] R. J. G. van Sloun, R. Cohen and Y. C. Eldar, "Deep Learning in Ultrasound Imaging," in Proceedings of the IEEE, vol. 108, no. 1, pp. 11-29, Jan. 2020.

[10] J. Wright, A. Ganesh, S. Rao, Y. Peng, and Y. Ma, "Robust principal component analysis: Exact recovery of corrupted low-rank matrices via convex optimization," Proc. Neural Inf. Process. Syst, pp. 1–9, 2009.

[11] E. J. Candes, X. Li, Y. Ma, and J. Wright, "Robust principal component analysis?" Journal of the ACM, vol. 58, no. 3, pp. 1–37, May 2011.

[12] M. Bayat and M. Fatemi, "Concurrent clutter and noise suppression via low rank plus sparse optimization for non-contrast ultrasound flow doppler processing in microvasculature," in Proc. IEEE Int. Conf. Acoust., Speech Signal Process. (ICASSP), Calgary, Canada, April 2018.

[13] O. Michailovich, A. Basarab, and D. Kouame, "Iterative reconstruction of medical ultrasound images using spectrally constrained phase updates," in Proc. IEEE 16th Int. Symp. Biomed. Imag. (ISBI), April 2019, pp. 1765–1768.

[14] S. Boyd, N. Parikh, E. Chu, B. Peleato, J. Eckstein, "Distributed Optimization and Statistical Learning via the Alternating Direction Method of Multipliers", Found. Trends Mach. Learn, 2010.

[15] P.L. Combettes, JC. Pesquet, "Proximal Splitting Methods in Signal Processing", Fixed-Point Algorithms for Inverse Problems in Science and Engineering. Springer Optimization and Its Applications, vol 49. Springer, pp.185-206, 2011.

[16] P. C. Hansen, J. G. Nagy, and D. P. O'leary, *Deblurring images: matrices, spectra, and filtering*, Society for Industrial and Applied Mathematics, 2006.